Available online at www.sciencedirect.com
SCIENCE DIRECT®

Applied Mathematics Letters 18 (2005) 1389–1395

Applied Mathematics Letters

www.elsevier.com/locate/aml

Hadamard expansions for integrals with saddles coalescing with an endpoint

R.B. Paris[a,*], D. Kaminski[b]

[a]*Division of Mathematical Sciences, University of Abertay Dundee, Dundee DD1 1HG, United Kingdom*
[b]*Department of Mathematics and Computer Science, University of Lethbridge, Lethbridge, Alberta, Canada T1K 3M4*

Received 3 September 2004; accepted 21 February 2005

Abstract

Hadamard expansions are constructed for Laplace-type integrals containing a parameter and an asymptotic variable x, which may be real or complex. These expansions yield a method of hyperasymptotic evaluation that remains valid throughout a range of the parameter corresponding to coalescence of a saddle point with an endpoint of the integration path. Numerical examples are given to illustrate the practical aspects of the computations.

Keywords: Hadamard expansions; Coalescing saddle; Hyperasymptotics; Incomplete gamma functions; Laplace-type integrals

1. Introduction

Hadamard expansions have featured in a recent article in this journal [1] and, with a straightforward modification, have been applied by the authors to the high-precision computation of functions defined by both integrals and differential equations — see [2,3] and [4]. This note describes some practical matters surrounding the computation of Hadamard expansions of functions defined by integrals in settings where saddle points of the integrand depend on a parameter and may coincide with an endpoint of the interval of integration, which itself may be a saddle point. The discussion is illustrated by treating two concrete examples which involve a finite integration path. These could have been chosen to involve infinite or

* Corresponding author. Tel.: +44 01382 308618; fax: +44 01382 308627.
E-mail addresses: r.paris@abertay.ac.uk (R.B. Paris), kaminski@cs.uleth.ca (D. Kaminski).

0893-9659/$ - see front matter © 2005 Elsevier Ltd. All rights reserved.
doi:10.1016/j.aml.2005.02.024

semi-infinite integration contours, but we have elected to construct examples that focus primarily on the coalescing saddle phenomenon.

2. Saddle coalescing with an endpoint

We begin with the function defined by the integral

$$I_1(x;a)=\int_0^1 \mathrm{e}^{-x\psi(t)}\mathrm{d}t, \qquad \psi(t)=\frac{1}{3}t^3+t^2-a\left(\frac{1}{2}t^2+2t\right)+\phi(a), \tag{1}$$

where the parameter a is assumed to be real and nonnegative and $\phi(a)=\frac{1}{6}a^3+a^2$ has been chosen so that $\psi(a)=0$. The "phase" function is seen to have saddles at $t=-2$ and $t=a$, so that in the small-a limit, the saddle at $t=a$ coalesces with the endpoint $t=0$ of the interval of integration. The argument x may be complex, so that $I_1(x)\equiv I_1(x;a)$ is seen to be an entire function of x for all a.

If $\mathrm{Im}(x)\neq 0$, then the path of integration $[0,1]$ can be rewritten as a sum of three steepest descent contours. If $0<\theta=\arg x<\pi$, this sum comprises a steepest descent contour issuing from the origin out to $\infty\mathrm{e}^{(2\pi/3-\theta/3)\mathrm{i}}$, followed by a steepest descent curve starting at $\infty\mathrm{e}^{(2\pi/3-\theta/3)\mathrm{i}}$, passing through the saddle at $t=a$ and ending at $\infty\mathrm{e}^{-\mathrm{i}\theta/3}$, the last curve in the sum being the steepest descent curve beginning at $\infty\mathrm{e}^{-\mathrm{i}\theta/3}$ and ending at the point $t=1$. If instead we have $-\pi<\arg x<0$, then a similar sum of steepest descent curves can be used, this time being the path from the origin to $\infty\mathrm{e}^{(-2\pi/3-\theta/3)\mathrm{i}}$, the steepest descent curve from $\infty\mathrm{e}^{(-2\pi/3-\theta/3)\mathrm{i}}$ passing through the saddle $t=a$ and ending in the valley $\infty\mathrm{e}^{-\mathrm{i}\theta/3}$, followed by the steepest descent path from $\infty\mathrm{e}^{-\mathrm{i}\theta/3}$ to the point $t=1$. For $\theta=0$, i.e., positive x, the interval $[0,1]$ is the steepest descent path through $t=a$ and furthermore, this path continues on to the saddle point $t=-2$, not directly involved in the definition of $I_1(x)$.

Let us first consider the special case of $x>0$. To develop a Hadamard expansion, we render the integral in the form of a Laplace transform, using the change of variable $u=\psi(t)$:

$$I_1(x)=-\int_a^0 \mathrm{e}^{-x\psi(t)}\mathrm{d}t+\int_a^1 \mathrm{e}^{-x\psi(t)}\mathrm{d}t=\left\{-\int_0^{\psi(0)}+\int_0^{\psi(1)}\right\}\mathrm{e}^{-xu}\frac{\mathrm{d}t}{\mathrm{d}u}\mathrm{d}u.$$

Inversion of the change of variable is controlled by the presence of the saddle $t=-2$, so that, for $0\le a<1$, the series in u obtained by inversion will converge in a disc centered at $u=0$ of radius $\omega=|\psi(-2)-\psi(a)|=\frac{4}{3}+\phi(a)+2a$. For each integral (using a '$-$' superscript for $t<a$ and a '$+$' superscript for $t>a$) we invert to find

$$\frac{\mathrm{d}t^{\pm}}{\mathrm{d}u}=\sum_{k=0}^{\infty}\frac{(\pm)^{k-1}c_k}{\Gamma(k/2+1/2)}u^{(k-1)/2}, \qquad c_0=\left(\frac{\pi}{2\psi''(a)}\right)^{1/2}, \tag{2}$$

and upon introducing the further scalings $u=\psi(0)v\equiv\omega_0 v$ in the first integral and $u=\psi(1)v\equiv\omega_1 v$ in the second integral, we obtain

$$\begin{aligned}I_1(x)=&-\int_0^1 \mathrm{e}^{-x\omega_0 v}\sum_{k=0}^{\infty}\frac{c_k(-1)^{k-1}\omega_0^{(k+1)/2}}{\Gamma(k/2+1/2)}v^{(k-1)/2}\mathrm{d}v\\&+\int_0^1 \mathrm{e}^{-x\omega_1 v}\sum_{k=0}^{\infty}\frac{c_k\omega_1^{(k+1)/2}}{\Gamma(k/2+1/2)}v^{(k-1)/2}\mathrm{d}v.\end{aligned}$$

We interchange integration and summation and evaluate the resulting integrals in terms of the normalised incomplete gamma functions P,

$$P(\alpha, z) = \frac{\gamma(\alpha, z)}{\Gamma(\alpha)} = \frac{1}{\Gamma(\alpha)} \int_0^z \mathrm{e}^{-t} t^{\alpha-1} \mathrm{d}t, \qquad (\mathrm{Re}(\alpha) > 0),$$

to arrive at the (absolutely convergent) Hadamard expansion, for $x > 0$:

$$I_1(x) = \sum_{k=0}^{\infty} \frac{(-)^k c_k}{x^{(k+1)/2}} P\left(\frac{1}{2}k + \frac{1}{2}, \omega_0 x\right) + \sum_{k=0}^{\infty} \frac{c_k}{x^{(k+1)/2}} P\left(\frac{1}{2}k + \frac{1}{2}, \omega_1 x\right) \equiv S_0(x) + S_1(x). \quad (3)$$

Notice that as $a \to 0^+$, the factor $\omega_0 = \phi(a)$ in the second argument of the first incomplete gamma function tends to 0, whilst $\omega_1 = \frac{4}{3} + \phi(a) - \frac{5}{2}a$ in the second incomplete gamma function tends to $\frac{4}{3}$. Provided $0 \le a < 1$, we have both ω_0 and $\omega_1 \le \omega$. There is one value $a^* \approx 0.54407$ in our a-interval where $\omega_0 = \omega_1$. For $0 \le a < a^*$, we have $\omega_0 < \omega_1$ with the reverse inequality holding when $a^* < a < 1$.

A crucial point is that the two series in (3) display differing convergence rates in the limit $a \to 0^+$, which in turn affects how the expansion is evaluated in numerical computation. By considering the growth of the coefficients c_k in (2), it can be shown that $c_k \sim k^{-3/2} \omega^{-k/2} \Gamma\left(\frac{1}{2}k + \frac{3}{2}\right)$ as $k \to \infty$. This last result, when combined with the behaviour $P(\alpha, x) \sim \mathrm{e}^{-x} x^\alpha / \Gamma(1+\alpha)$ for large α and fixed x, then shows that the late terms ($k \gg 1$) in $S_j(x)$ possess the behaviour

$$\mathrm{e}^{-\omega_j x} k^{-3/2} (\omega_j/\omega)^{k/2} \qquad (k \to \infty;\ j = 0, 1). \quad (4)$$

Then, as $a \to 0^+$, the convergence of $S_0(x)$ is rapid while that of $S_1(x)$ is associated with a slow algebraic decay essentially controlled by $k^{-3/2}$. This latter series benefits dramatically from the modification process detailed in [2].

The modified expansion for the Hadamard series $S_j(x)$ consists of truncation after m_0 terms and rearrangement of the tail in the form

$$S_j(x) = \sum_{k=0}^{m_0-1} \frac{(-)^{(j-1)k} c_k}{x^{(k+1)/2}} P\left(\frac{1}{2}k + \frac{1}{2}, \omega_j x\right) + \mathrm{e}^{-\omega_j x} \sum_{r=0}^{\infty} \sigma_{rj} (\omega_j x/m_0)^r, \quad (5)$$

where the truncation index m_0 is free to be chosen and the coefficients $\sigma_{rj} \equiv \sigma_{rj}(m_0)$ (which are independent of x) are specified by

$$\sigma_{rj} = m_0^r \left\{ \frac{1}{r!} \int_{\alpha_j}^{\beta_j} (1 - \psi(t)/\omega_j)^r \mathrm{d}t - \sum_{k=0}^{m_0-1} \frac{(-)^{(j-1)k} c_k \omega_j^{(k+1)/2}}{\Gamma\left(\frac{1}{2}k + r + \frac{3}{2}\right)} \right\}$$

with $(\alpha_0, \beta_0) = (0, a)$ and $(\alpha_1, \beta_1) = (a, 1)$. Provided m_0 is chosen so that $\omega_j x/m_0 < 1$, the terms in the tail are found numerically to decay very rapidly thereby overcoming the slow algebraic decay of the unmodified Hadamard series. In numerical computations, the sum in (5) over r is truncated after $r_0 + 1$ terms. It is important to stress that the modified Hadamard expansion in (5) is still exact and that no approximation has been introduced.

In Fig. 1, we show the decay of the terms (on a $\log_{10}$ scale) of the two series in (3) for a small value of the parameter a when $x = 5$. The coefficients c_k were computed by numerical inversion using *Mathematica*. In accordance with the estimate (4), the terms in $S_0(x)$ in Fig. 1(a) decay very rapidly

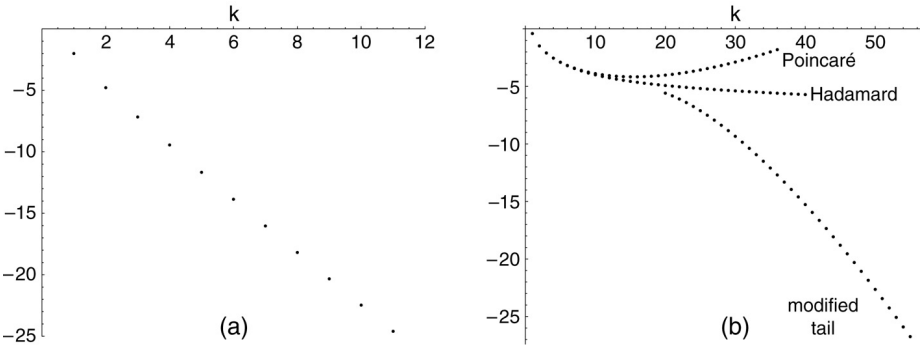

Fig. 1. Decay of terms in the Hadamard expansion for $I_1(x;a)$ when $x = 5$ and $a = 10^{-2}$ plotted as ordinal value of the term vs. $\log_{10}$ of the absolute value of the term: (a) the terms in $S_0(x)$ and (b) the terms in the associated Poincaré asymptotic expansion (top), the unmodified Hadamard series (middle) and the modified tail (bottom) for $S_1(x)$.

Table 1
Absolute values of the errors in the computation of $I_1(x;a)$ for different values of a with $x = 10$ (left half of table) and for different values of θ with $a = 10^{-2}$ (right half of table) when $x = 10\mathrm{e}^{\mathrm{i}\theta}$ for truncation indices $m_0 = 40$ and $r_0 = 20$ or 30

a	|Error| ($\theta = 0$ fixed)		θ/π	|Error| ($a = 10^{-2}$ fixed)	
	$r_0 = 20$	$r_0 = 30$		$r_0 = 20$	$r_0 = 30$
10^{-1}	8.119×10^{-21}	6.701×10^{-26}	0	2.320×10^{-17}	6.361×10^{-23}
10^{-2}	2.320×10^{-17}	6.361×10^{-23}	0.25	9.175×10^{-16}	2.623×10^{-21}
10^{-4}	5.312×10^{-17}	1.752×10^{-22}	0.50	7.415×10^{-12}	2.234×10^{-17}
10^{-6}	5.356×10^{-17}	1.770×10^{-22}	0.75	6.254×10^{-12}	1.933×10^{-17}
0	5.356×10^{-17}	1.770×10^{-22}	1.00	5.910×10^{-12}	1.839×10^{-17}

Entries in the right half of the table corresponding to $\mathrm{Re}(x) < 0$ have been scaled by a factor of $\mathrm{e}^{x\psi(1)}$.

so that the above-mentioned modification process is not necessary in this instance. Fig. 1(b) shows the terms in the finite main sum of $S_1(x)$ together with those in its modified tail, which now can be seen to decay roughly at the same rate as the initial asymptotic-like phase of the main sum. Also shown in this figure is the behaviour of the associated Poincaré asymptotic expansion of the integral over the interval $[a, 1]$ — obtained from $S_1(x)$ by formally replacing the incomplete gamma function by unity — which presents the familiar initial decrease followed by ultimate divergence.

We display the results of numerical computations in the left half of Table 1 where the absolute error in the calculation of $I_1(x;a)$ by means of (3) is given for different values of a for fixed x, with the exact value found by numerical quadrature. We take $x = 10$ and employ the *fixed* truncation indices $m_0 = 20$, $r_0 = 20$ or 30 for $S_1(x)$ and up to a maximum of 20 terms (according to the value of a) for $S_0(x)$.

Following the discussion in [2], when x becomes complex the approach to take would be to represent I_1 as a sum of steepest descent contours and then proceed to construct Hadamard expansions associated with each contour integral [3]. This process produces series where the associated incomplete gamma functions have arguments that are positive, guaranteeing that the functions P have the desirable 'cut-off' property of dropping quickly and monotonically from 1 to 0 as k increases, which in turn produces the most rapid possible convergence for the expansion.

If we are willing to obtain slightly less rapidly converging series, then much of the computational cost of the above path decomposition can be avoided. Furthermore, the approach taken in developing (3)

works without modification if x is allowed to be complex. The expansion (3) will, however, now involve incomplete gamma functions whose arguments $\omega_j x$ are complex. Although this will result in a loss of their simple smoothing property, these functions still decay as k increases. In the right half of Table 1 we show results for complex x when $a = 10^{-2}$ using the same truncation indices.

3. Saddle coalescing with an endpoint saddle

Our second example modifies the situation for I_1 by considering a saddle that coalesces with an endpoint that is itself a saddle. To illustrate this setting, we take $a \geq 0$ and consider

$$I_2(x;a) = \int_0^1 \mathrm{e}^{-x\psi(t)}\mathrm{d}t, \qquad \psi(t) = \frac{1}{4}t^4 + \frac{1}{3}t^3 - a\left(\frac{1}{3}t^3 + \frac{1}{2}t^2\right) + \phi(a), \tag{6}$$

where $\phi(a) = \frac{1}{12}a^4 + \frac{1}{6}a^3$ is chosen so that again $\psi(a) = 0$. The integral $I_2(x) \equiv I_2(x;a)$ now has three saddle points at $t = 0$, $t = a$ and $t = -1$ (the "remote" saddle), and clearly, as $a \to 0^+$, the saddle at $t = a$ coalesces with the saddle at the left endpoint of the integration path, producing a double saddle in the limit.

The steepest descent path structure for I_2 is similar to that of I_1, except that now the left-most endpoint of the interval has a steepest descent path passing through it, and coalescence takes place in the $a \to 0^+$ limit. As before, let us take $x > 0$ initially in our deliberations, so that the interval $[0, 1]$ itself is the steepest descent path passing through $t = a$. We mention that the Hadamard expansions we obtain remain valid for complex values of x.

As in our first example, we decompose the integral $I_2(x;a)$ into two integrals taken over the intervals $[0, a]$ and $[a, 1]$. The first integral has saddle points at each endpoint, so that when we expand about $t = a$, the inversion process associated with the change of variable $u = \psi(t) - \psi(a) = \psi(t)$ will lead to an expansion for $\mathrm{d}t/\mathrm{d}u$ of the form (2), but now valid in the smaller disc $|u| < \omega_0 = \phi(a)$ due to the presence of the saddle at $t = 0$. Then, as in Section 2, the contribution from the interval $[0, a]$ produces the Hadamard expansion $S_0(x)$ in (3), with the coefficients c_k corresponding to $\psi(t)$ in (6).

For the integral over $[a, 1]$, it is no longer practical in the small-a limit to expand about the saddle $t = a$, since the associated radius of convergence ω_0 shrinks to zero as $a \to 0^+$. This would result in a sequence of many Hadamard expansions being required to cover the interval $[a, 1]$. To overcome this difficulty, we follow [5] and expand about the endpoint $t = 1$. With the change of variable $u = \psi(t) - \psi(1)$, we find the inversion $\mathrm{d}t/\mathrm{d}u = \sum_{k=0}^{\infty} b_k u^k/k!$, with $b_0 = 2(1-a)$, valid in the disc $|u| < \omega_1$ (where $\omega_1 = \psi(1)$) whose radius is controlled by the saddle at $t = a$. Substitution of this result into the integral over $[a, 1]$ yields

$$\int_a^1 \mathrm{e}^{-x\psi(t)}\mathrm{d}t = -\mathrm{e}^{-x\psi(1)}\int_0^{-\omega_1} \mathrm{e}^{-xu}\frac{\mathrm{d}t}{\mathrm{d}u}\,\mathrm{d}u = -\mathrm{e}^{-\omega_1 x}\sum_{k=0}^{\infty}\frac{b_k}{x^{k+1}}P(k+1, -\omega_1 x) \equiv S_2(x). \tag{7}$$

The Hadamard expansion for I_2 for $0 \leq a < 1$ is then given by $I_2(x;a) = S_0(x) + S_2(x)$. We remark that the series in (7) involves incomplete gamma functions with negative argument — this is an unavoidable consequence of our having expanded about the point $t = 1$. A discussion of the convergence of such series is given in [5]. In the special case $a = 0$, $S_0(x)$ vanishes and we are left with the single Hadamard expansion in (7) with $\omega_1 = \frac{7}{12}$. It is worth mentioning that if we had expanded about the double saddle at $t = 0$, the techniques of [2] would have resulted in a Hadamard expansion consisting

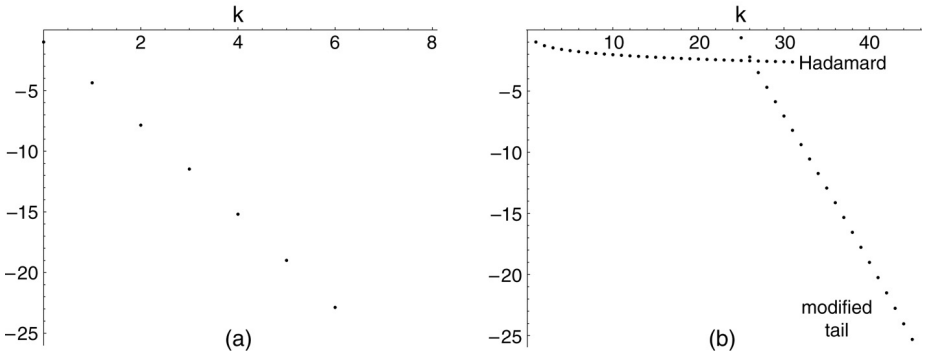

Fig. 2. Decay of terms in the Hadamard expansion for $I_2(x;a)$ when $x=5$ and $a=10^{-2}$ plotted as ordinal value of the term vs. $\log_{10}$ of the absolute value of the term: (a) the terms in $S_0(x)$ with $m_0=0$ and (b) the terms in (7) with $m_0=25$.

of four series, each series corresponding to incomplete gamma functions with arguments $\omega_j x$, where the ω_j are in turn $\frac{1}{12}$, $\frac{1}{12}$, $\frac{2}{12}$ and $\frac{3}{12}$.

Since the radius of convergence of the expansion (2) is ω_0, the decay of the terms in $S_0(x)$ will now be controlled by $k^{-3/2}$, with the result that the modified form of the expansion in (5) must be employed. The terms in the finite sum (truncated after m_0 terms), however, are found to decay very slowly as $a\to 0^+$; consequently it is better in this example to set $m_0=0$ and represent $S_0(x)$ by means of the rearranged tail in (5). The series in (7) is also employed in its modified form in a manner similar to that for $S_1(x)$. This takes the form [5]

$$S_2(x)=-\mathrm{e}^{-\omega_1 x}\sum_{k=0}^{m_0-1}\frac{b_k}{x^{k+1}}P(k+1,-\omega_1 x)+\sum_{r=0}^{\infty}\sigma_{r2}(-\omega_1 x/m_0)^r,$$

where

$$\sigma_{r2}=m_0^r\left\{\frac{1}{r!}\int_a^1(\psi(t)/\omega_1)^r\,\mathrm{d}t-\sum_{k=0}^{m_0-1}\frac{(-)^k b_k\omega_1^{k+1}}{(k+r+1)!}\right\}$$

and m_0 is chosen as in (5). An example of the decay of the terms in the Hadamard expansions $S_0(x)$ and $S_2(x)$ is displayed in Fig. 2. Numerical results for the computation of $I_2(x;a)$ at fixed (large) x and varying a are shown in Table 2. As for the first example considered, the expansion $I_2(x;a)=S_0(x)+S_2(x)$ remains valid for complex x: if we are prepared to accept less rapidly converging series, then again we can avoid the use of steepest descent paths and continue to employ the interval $[0,1]$ as integration path. The results for complex x obtained in this manner are also presented in Table 2.

4. Closing remarks

Our examples showcase the possibility of generating Hadamard expansions simpler than one expects through routine application of existing theory and further, that the expansions so obtained retain their validity for significant ranges of the parameter controlling the coalescence of the saddle with the endpoint. These simpler expansions can have incomplete gamma functions with negative argument, but as the numerics illustrate, high-precision computation is still a feature of these expansions. This remains the case even when the variable x moves into the complex plane and truncation indices remain fixed,

Table 2
Absolute values of the errors in the computation of $I_2(x;a)$ for different values of a with $x = 10$ (left half of table) and for different values of θ with $a = 10^{-2}$ (right half of table) when $x = 10e^{i\theta}$

a	|Error| ($\theta = 0$ fixed)		θ/π	|Error| ($a = 10^{-2}$ fixed)	
	$r_0 = 25$	$r_0 = 30$		$r_0 = 25$	$r_0 = 30$
10^{-1}	2.071×10^{-24}	1.949×10^{-29}	0	8.239×10^{-23}	1.559×10^{-27}
10^{-2}	8.239×10^{-23}	1.559×10^{-27}	0.25	8.478×10^{-23}	1.601×10^{-27}
10^{-4}	1.198×10^{-22}	2.434×10^{-27}	0.50	9.152×10^{-23}	1.717×10^{-27}
10^{-6}	1.203×10^{-22}	2.445×10^{-27}	0.75	1.001×10^{-22}	1.861×10^{-27}
0	1.203×10^{-22}	2.445×10^{-27}	1.00	1.044×10^{-22}	1.933×10^{-27}

The truncation indices employed are $m_0 = 0$, $r_0 = 10$ for $S_0(x)$ and $m_0 = 20$, $r_0 = 25$ or 30 for $S_2(x)$.

suggesting that these Hadamard expansions (with modified tails after truncation when necessary) are a robust computational tool in the hyperasymptotic evaluation of Laplace-type integrals.

Although we have concentrated on the situation $a \to 0^+$, it is possible to consider $a \to 0^-$. In the case of I_1 this results in the integral becoming exponentially small for large positive x and the saddle at $t = a$ lying just outside the range of integration $[0, 1]$. A computational scheme in this case would be to extract the exponential factor $e^{-x\phi(a)}$ and expand about $t = a$ to find

$$e^{x\phi(a)} I_1(x) = \left\{ \int_a^1 - \int_a^0 \right\} e^{-x\tilde{\psi}(t)} dt,$$

where $\tilde{\psi}(t) = \psi(t) - \phi(a)$. The first integral on the right-hand side will require two stages, since the radius of convergence of the expansion about $t = a$ will not cover the full range $[a, 1]$. Similar considerations apply to I_2. Finally, we remark that our uniform treatment of Laplace-type integrals by Hadamard expansions when the parameter $a \to 0$ has avoided the complication of the usual transformation of mapping $\psi(t)$ to either a quadratic or cubic polynomial; see, for example, [6, Chapter 7].

References

[1] S. Yang, H.M. Srivastava, Some generalizations of the Hadamard expansion for the modified Bessel function, Appl. Math. Lett. 17 (2004) 591–596.
[2] R.B. Paris, On the use of Hadamard expansions in hyperasymptotic evaluation of Laplace-type integrals. I: real variable, J. Comput. Appl. Math. (167) (2004) 293–319.
[3] R.B. Paris, On the use of Hadamard expansions in hyperasymptotic evaluation of Laplace-type integrals. II: complex variable, J. Comput. Appl. Math. (167) (2004) 321–343.
[4] D. Kaminski, R.B. Paris, On the use of Hadamard expansions in hyperasymptotic evaluation: differential equations of hypergeometric type, Proc. Roy. Soc. Edinburgh 134A (2004) 159–178.
[5] R.B. Paris, Exactification of the method of steepest descents: the Bessel functions of large order and argument, Proc. R. Soc. Lond. 460A (2004) 2737–2759.
[6] R. Wong, Asymptotic Expansion of Integrals, Academic Press, London, 1989.